Colloids and Surfaces B: Biointerfaces 84 (2011) 454–461

Contents lists available at ScienceDirect

Colloids and Surfaces B: Biointerfaces

journal homepage: www.elsevier.com/locate/colsurfb

A glucose biosensor based on chitosan–Prussian blue–multiwall carbon nanotubes–hollow PtCo nanochains formed by one-step electrodeposition

Xin Che, Ruo Yuan*, Yaqin Chai, Jingjing Li, Zhongju Song, Wenjuan Li, Xia Zhong

Key Laboratory on Luminescence and Real-Time Analysis, Ministry of Education, College of Chemistry and Chemical Engineering, Southwest University, Chongqing 400715, China

ARTICLE INFO

Article history:
Received 23 September 2010
Received in revised form 2 January 2011
Accepted 28 January 2011
Available online 3 February 2011

Keywords:
Chitosan
Prussian blue
Multiwall carbon nanotubes
Hollow PtCo nanochains
Glucose
Electrodeposition

ABSTRACT

In this paper, a simple one-step electrodeposition method is described to fabricate chitosan–Prussian blue–multiwall carbon nanotubes–hollow PtCo nanochains (CS–PB–MWNTs–H-PtCo) film onto the gold electrode surface, then glucose oxidase (GOD) and Nafion were modified onto the film subsequently to fabricate a glucose biosensor. The morphologies and electrochemistry of the composite were investigated by using Fourier transform infrared (FTIR) spectrometry, scanning electron microscopy (SEM) and electrochemical techniques including cyclic voltammetry (CV) and electrochemical impedance spectroscopy (EIS), respectively. The performances of the biosensor have been investigated by chronoamperometry method under the optimized conditions. This biosensor showed a linear response to glucose range from 1.5 μM to 1.12 mM with a detection limit of 0.47 μM (S/N = 3), a high sensitivity of 23.4 $\mu A\,mM^{-1}\,cm^{-2}$, and a fast response time. The apparent Michaelis–Menten constant (K_M^{app}) was 1.89 mM. In addition, the biosensor also exhibited strong anti-interference ability, excellent stability and good reproducibility.

1. Introduction

For the treatment and control of diabetes, the amount of blood glucose has to be detected. For this reason, the glucose biosensor is the most extensively studied and researched among many different types of enzyme-based biosensors [1]. And glucose oxidase (GOD) is widely employed because of its good stability and relatively inexpensive [2,3]. It can catalyze the electron transfer from glucose to oxygen accompanying the production of hydrogen peroxide (H_2O_2) and gluconolactone. Therefore, the glucose concentration can be monitored indirectly by the oxidation current of H_2O_2 [4]. But a limitation is the severe interference caused by reducing agents such as ascorbic acid, acetaminophen or uric acid in clinical application since the electrode must be poised at high positive working potentials for electrochemical detection of H_2O_2 [5,6]. To solve this problem, Prussian blue (PB) has been introduced to work as a redox mediator to reduce the operating potential drastically, and offer the most sensitive and interference free detection [7].

PB, whose composition is expressed as $FeIII_4[FeII(CN)_6]_3$, is considered as an "artificial peroxidase"due to its high activity and selectivity toward the reduction of H_2O_2 and it has been extensively used in the construction of electrochemical biosensors [8]. In recent years, many investigations have focused on the synthesis of nano-sized PB particles and many methods including microemulsion [9], polymer protection [10] have been advocated. However, the methods mentioned above are time-consuming or technically complex and the as-prepared nanoparticles are not very stable in some degree for a long time. Thus, it is very important to find a rapid and convenient method to synthesize PB nanoparticles to eliminate the problems. Compared with the traditional techniques, electrodeposition is a facile, versatile and simple method to prepare fresh PB film with controllable thickness and good reproducibility [11,12]. But an alone electrodeposited PB film is prone to decompose and exhibits poor cycling stability at physiological pH due to the attack of hydroxide ions, which limit its employment in biosensor fabrication [4,13]. Therefore, chitosan (CS) has been successfully introduced to prevent the leakage of PB and improve the stability of the biosensor.

CS is a polysaccharide derived by deacetylation of biopolymer chitin [14]. Chitosan's pK_a is about 6.3 because of some primary amino groups, CS is protonated and soluble at lower pH solutions ($<pK_a$). When the pH is higher than pK_a, the amino groups become deprotonated and form an insoluble hydrogel network [15,16]. Based on its attractive biocompatible, biodegradable, nontoxic and excellent film-forming ability, chitosan hydrogel was electrochemically deposited onto electrode surface with PB to form CS–PB hybrid film [17]. At the same time, other substances such as metal nanoparticles [11,18] or carbon nanotubes [19] can be effectively incorporated to form a composite during the electrodeposition to enhance electrical conductivity and improve the microarchitecture.

* Corresponding author. Tel.: +86 23 68252277; fax: +86 23 68253172.
E-mail addresses: chexingg-613@163.com (X. Che), yuanruo@swu.edu.cn (R. Yuan).

0927-7765/$ – see front matter © 2011 Elsevier B.V. All rights reserved.
doi:10.1016/j.colsurfb.2011.01.041

Since multi-wall carbon nanotubes (MWNTs) were discovered in 1991 by Iijima, they have been widely used in electrochemical biosensor due to their unique properties, such as high electrical conductivity, mechanical strength and chemical stability and so on [20,21]. Moreover, MWNTs possess high surface-to-volume ratio and strong adsorptive ability [22]. When MWNTs were incorporated into CS–PB hybrid film, the CS–PB–MWNTs composite can form a random mesh on the electrode surface of high catalytic surface area.

On the other hand, electrochemical behavior and applications of nanoparticles have attracted considerable interest in the past few years [23]. Introducing metal nanoparticles especially hollow metal nanoparticles into electrode surfaces has developed various electrochemical biosensors since the nanoparticles have high catalytic activities for many chemical reactions [24]. But most reported hollow spheres are generally fabricated by template-directed synthesis [25] or emulsion synthesis [26,27] which were technically complicated. Simultaneously, it is a challenge to retain the shell structures during core removal. Thus, the one-pot synthesis of hollow nanostructured materials was carried out by the galvanic displacement reaction, which is fast, simple and one-step solution route for the preparation of hollow nanostructures [28]. Accordingly, hollow PtCo (H-PtCo) nanochains were synthesized by employing Co nanoparticles produced in situ as a template. The performance of the glucose biosensor was improved with the introducing of H-PtCo nanochains, because they can not only facilitate the transfer of electron but also have high catalytic activities for glucose oxidation. Meanwhile, the porous high surface area CS–PB–MWNTs–H-PtCo film provided a high loading capacity for glucose oxidase.

In this paper, a new glucose biosensor was constructed based on electrochemical deposition of CS–PB–MWNTs–H-PtCo composite on a gold electrode as a mediator. After GOD was immobilized onto the film, Nafion was dipped on GOD/CS–PB–MWNTs–H-PtCo membrane to maintain the stability of modified electrode. This strategy has following advantages. Firstly, one-step electrochemical co-deposition is a clean and quick method to fabricate the CS–PB–MWNTs–H-PtCo composite film. Secondly, incorporating MWNTs and H-PtCo nanochains into CS–PB hybrid film increased electron transfer and improved the microarchitecture of the electrode surface. Attribute to the synergistic effects between PB particles, MWNTs and H-PtCo nanochains, the biosensor exhibited a high electrocatalytic activity to glucose. Finally, Nafion film used here prevented the loss of the enzyme molecules, improved the anti-interference ability of the biosensor and provided a biocompatible microenvironment to maintain enzymatic activity. In addition, the influence of pH value, applied potential and deposition time on the biosensor performance was evaluated. The resulted biosensor exhibited high sensitivity, good reproducibility, long-term stability and short response time.

2. Experiment

2.1. Reagents and apparatus

MWNTs (>95% purity) were obtained from Chengdu Organic Chemicals Co. Ltd. of the Chinese Academy of Science and purified by fluxing in concentrated nitric acid for 7 h prior to use. Hydrogen hexachloroplatinate (IV) hexahydrate ($H_2PtCl_6{\cdot}6H_2O$, 99%), glucose oxidase (E.C 1.1.3.4, 151,000 unit/g), chitosan (CS, deacetylating grade: 70–85%) were all purchased from Sigma. Glucose stock solution was stored to mutarotate for 24 h at room temperature before using. Other reagents were of analytical reagent grade. All solutions were prepared with doubly distilled water. The phosphate buffer (PBS) containing 0.025 M KH_2PO_4, 0.025 M K_2HPO_4 and 0.1 M KCl was chosen as the supporting electrolyte.

Cyclic voltammetry (CV) and electrochemical impedance spectroscopy (EIS) studies were performed using CHI 660D electrochemistry workstation (Shanghai CH Instruments Co., China). Infrared spectra were collected with a Fourier transform infrared spectrophotometer (GX, Perkin Elmer Co., USA) using KBr disks. The structure of H-PtCo nanochains was investigated with JEM-100CXII transmission electron microscopy (TEM, Japan). Scanning electron micrographs were studied by scanning electron microscope (SEM, S-4800, Hitachi, Japan).

2.2. Synthesis of hollow PtCo nanochains

Hollow PtCo nanochains (H-PtCo) were synthesized according to Ref. [29] by a little change. The synthesis process was described as follows. Firstly, 50 mL aqueous solution containing $CoCl_2{\cdot}6H_2O$ (8.5 mg) and PVP (100 mg) was deaerated with N_2 for 15 min. Then, freshly prepared $NaBH_4$ (10 mg in 20 mL of H_2O) was added dropwise. After all of the $NaBH_4$ has been added, 17 mL of H_2PtCl_6 was added immediately under vigorous stirring. Then the color of the solution became blackish brown. After half an hour, the product was collected by centrifugation, washed several times with H_2O and ethanol. For comparison, solid PtCo nanoparticles (S-PtCo) were prepared according to the literature [30]. The same amount of PVP, $CoCl_2{\cdot}6H_2O$ and H_2PtCl_6 used above were mixed simultaneously under magnetic stirring. Then $NaBH_4$ as reducer was added dropwise. Finally, the products were dried under ambient conditions for further use.

2.3. Preparation of the electrodeposition base solution

Chitosan solution (0.05%) (w/v) was prepared by dissolving 50 mg CS powder in 100 mL 1.0% acetic acid solution and stirred at room temperature until CS powder dissolve completely. Then the solution was stored at 4 °C when not in use.

Before the experiment, MWNTs (2 mg L^{-1}) and hollow PtCo nanochains (2 mg L^{-1}) were dispersed into chitosan solution to give a homogeneous dispersion and noted as solution A; a solution containing 5 mM $FeCl_3$, 5 mM $K_3[Fe(CN)_6]$, 0.2 M KCl, 0.02 M HCl and 0.05% CS was prepared as solution B. Before electrodepositing, the solution A was freshly mixed with solution B under stirring condition (v/v = 1:1) to form the electrodeposition base solution.

2.4. Preparation of glucose biosensor

The gold electrode (Au, Φ = 4 mm) was polished with 0.3 and 0.05 μm alumina slurry, respectively. After rinsed with distilled water, the electrode was chemically cleaned by immersing into freshly prepared "piranha" solution (7:3 (v/v) mixture of concentrated H_2SO_4 and 30% H_2O_2) for 30 s and followed by sonicating in ethanol and water successively for 5 min.

After the electrode was dried in air, the clean gold electrode was immersed into the freshly prepared electrodeposition base solution under slightly stirring and electrodeposited for 300 s with a constant potential of +0.4 V (vs. SCE). Following that, the modified electrode was transferred into 0.01 M HCl/0.1 M KCl solution, and electrochemically scanned for 25 circles between −0.05 V and 0.35 V at a scan rate of 50 mV s^{-1} to obtain CS–PB–MWNTs–H-PtCo/gold electrode. After the modified electrode was dried in air, 10 μL 5 mg mL^{-1} GOD was added onto the film. Finally, the GOD/CS–PB–MWNTs–H-PtCo modified gold electrode was coated with an extra 3.0 μL 0.5% Nafion to maintain the stability of modified electrode. The schematic illustration of the stepwise procedure of the biosensor fabrication was shown in Fig. 1.

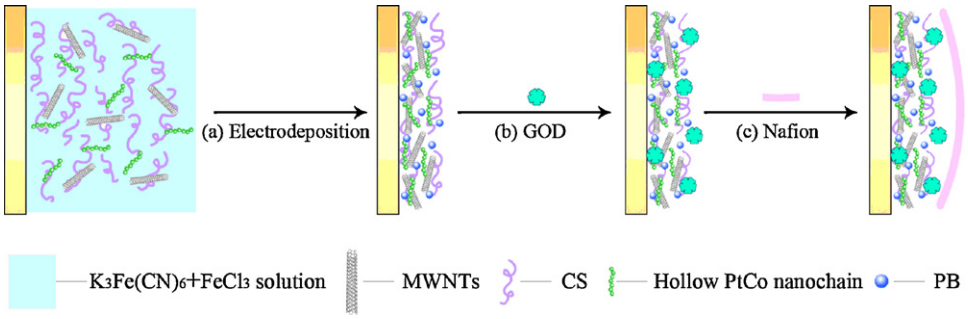

Fig. 1. Illustration of the preparation process of the glucose biosensors.

For comparison, Nafion/GOD/CS–PB/Au Nafion/GOD/CS–PB–MWNTs/Au, Nafion/GOD/CS–PB–H-PtCo/Au and Nafion/GOD/CS–PB–MWNTs–S-PtCo/Au electrodes were fabricated by the similar procedures. All enzyme electrodes were stored in refrigerator (4 °C) when not in use.

2.5. Experimental measurements

Electrochemical experiments were performed in a conventional electrochemical cell containing a three-electrode cell, in which a modified gold electrode, a saturated calomel electrode and a platinum wire served as the working, reference and auxiliary electrodes, respectively. A 0.025 M PBS (pH 6.0) including 0.1 M KCl was used as electrolyte solution. The stepwise assembly of the biosensor was characterized by electrochemical impedance spectroscopy (EIS) and cyclic voltammetric (CV). EIS was carried out in the presence of a 5 mM $K_3[Fe(CN)_6]/K_4[Fe(CN)_6]$ (1:1) mixture as redox probe in 0.025 M PBS (pH 6.0) containing 0.1 M KCl. The alternative voltage was 5 mV and the frequency range was 50 MHz–10 kHz. The CV was carried out with the potential range from −0.2 to 0.5 V under a sweeping rate of 100 mV s^{-1}. Amperometric measurements were carried out in a 5 mL stirred PBS at room temperature with an applied potential of −0.1 V. Different concentrations of β-D-glucose solution were added when background current reached a constant value. All potentials were measured and reported vs. the SCE.

3. Results and discussion

3.1. SEM characterizations of CS–PB–MWNTs–H-PtCo composite film and TEM characterization of hollow PtCo nanochains

In order to verify the successful assembly of CS–PB–MWNTs–H-PtCo nanocomposite film, the morphologies of the CS–PB, CS–PB–MWNTs and CS–PB–MWNTs–H-PtCo composite on a gold substrate were characterized by SEM (Fig. 2).

As seen from Fig. 2A, a compact CS–PB film with lots of small PB particles formed on the gold surface. After MWNTs added, a relatively rough mesh was seen in Fig. 2B. When MWNTs and hollow PtCo nanochains were incorporated into the CS–PB film, we can see a rougher and more porous surface. Simultaneously, the morphology possessed a three-dimensional structure in some degree. Compared with the CS–PB and CS–PB-MWNTs film, the CS–PB–MWNTs–H-PtCo modified electrode had larger active surface area (Fig. 2C). Thus, the electrode had an excellent conductivity.

The microstructure of hollow PtCo nanochains was also observed by TEM (Fig. 2D). The contrast between the dark edge and the bright center provided convincing evidence of the hollow structure. An average diameter of the hollow spheres was determined to be 7 nm. Isolated hollow nanoparticles were not observed out of the nanochains, suggesting that they are robust enough to survive centrifugation and ultrasonic treatment.

3.2. Electrochemical impedance spectroscopy (EIS) and cyclic voltametry (CV) characterization of the modified electrode

EIS was used to characterize the stepwise assembly of the biosensor since it was an effective method to probe the interface properties of surface-modified electrodes. The linear part, observed in the EIS, represents the diffusion-limited process. The semicircle portion in EIS corresponds to the electrontransfer-limited process. The electron transfer resistance (R_{et}) at electrode surface is equal to the semicircle diameter. Therefore, the stepwise assembly of the biosensor was characterized by EIS, and the results are shown in Fig. 3A. As can be seen, curve a presented a small semicircle domain implying a low R_{et} = 97 Ω on the bare gold electrode. When CS–PB–MWNTs–H-PtCo composite was deposited onto the electrode surface, the electron transfer resistance decreased dramatically to 24 Ω (curve b), the reason maybe that the excellent conductivity of CS–PB–MWNTs–H-PtCo composite have porous network-like structure, and have larger effective surface area than the bare electrode surface. After GOD was modified on CS–PB–MWNTs–H-PtCo/Au electrode, the EIS presented an apparent increase and the electrontransfer resistance was 272 Ω (curve c), which was due to the inhibition effect of the macromolecules for electron transfer. The electrontransfer resistance further increased to 641 Ω when non-conductive properties of Nafion covered onto the GOD/CS–PB–MWNTs–H-PtCo film (curve d).

Meanwhile, CV has also been employed to characterize the assembly process of the modified electrode (Fig. 3B). The image showed the CV of bare gold electrode (curve a), in which no peak was observed as a result of the lack of redox-active material. After the electrode was electrodeposited in the electrodeposition base solution, a pair of well-defined redox peaks was observed (curve b), indicating that PB had been assembled on the electrode surface through electrochemical co-deposition. The anodic and cathodic peaks decreased gradually when GOD (curve c) and Nafion (curve d) were modified onto CS–PB–MWNTs–H-PtCo composite modified gold electrode, respectively. The results indicated that GOD and Nafion had been successfully immobilized on the electrode surface.

CVs of the proposed biosensor at different scan rates were also recorded (Fig. 4).

It can be seen that the peak currents increased with the scan rates in the range of 10–400 mV s^{-1}. Square root of scan rate showed a linear relation with peak current (shown in the inset of Fig. 4), indicating a diffusion-controlled behavior of the biosensor.

3.3. The electrical conductivity of CS–PB–MWNTs–H-PtCo composite

In order to investigate the enhanced electrical conductivity of CS–PB–MWNTs–H-PtCo composite because of the introduction of

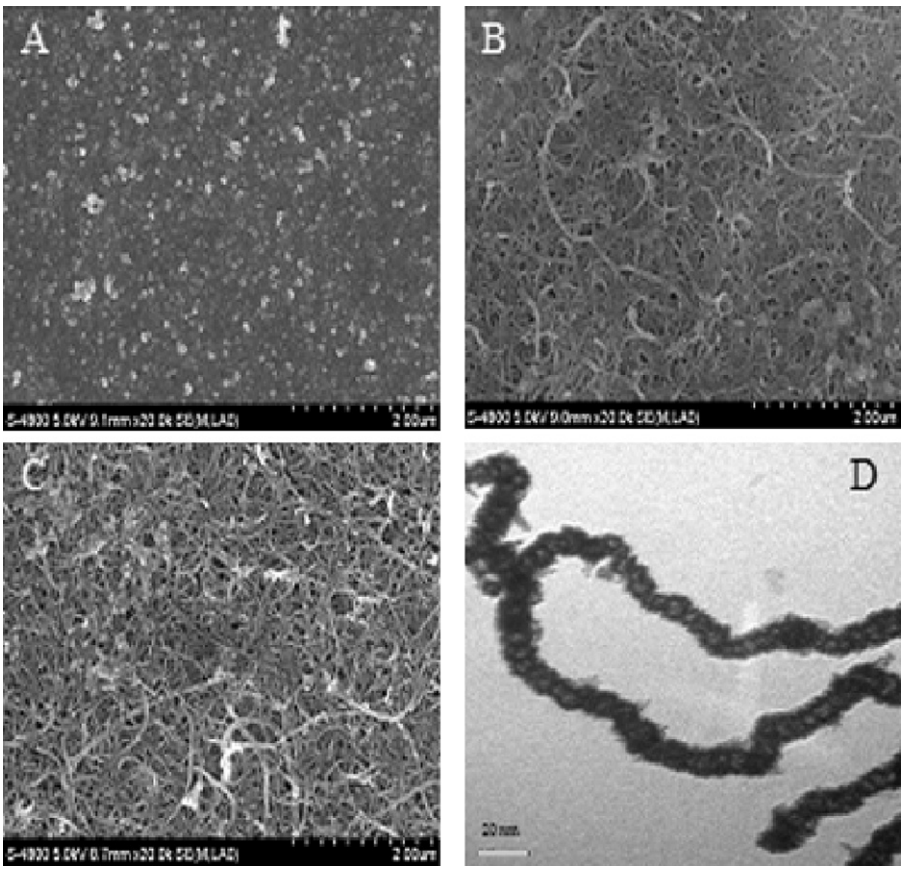

Fig. 2. SEM images of (A) CS–PB hybrid film; (B) CS–PB–MWNTs film; (C) CS–PB–MWNTs–H-PtCo nanocomposite film and (D) TEM images of hollow PtCo nanochains.

MWNTs and hollow PtCo nanochains, CV and EIS measurements were used to the contrast tests (Fig. 5).

As shown in Fig. 5A, with incorporating of MWNTs and hollow PtCo nanochains into the CS–PB hybrid film, the peak current of CS–PB–MWNTs–H-PtCo/Au was obviously higher than that of CS–PB/Au, CS–PB–H-PtCo/Au and CS–PB–MWNTs/Au. Moreover, the resistance of CS–PB–MWNTs–H-PtCo/Au was smaller than that of the electrodes without MWNTs or H-PtCo nanochains (Fig. 5B). The results indicated that MWNTs and H-PtCo nanochains improved the conductivity of composite, which could enhance the performance of biosensor. Fourier transform infrared (FTIR) was further applied to characterize the formation and properties of the CS–PB–MWNTs composite film (Fig. 1S).

3.4. Influence of pH and applied potential on biosensor response

The pH value is one of the parameters which affect the performance of the glucose biosensor. The change of chronoamperometric current with the pH under constant glucose concentration (0.3 mM) was shown in Fig. 6.

The results show that the maximum response appears at pH 6.0. Simultaneously, the stability of CS–PB–MWNTs–H-PtCo compos-

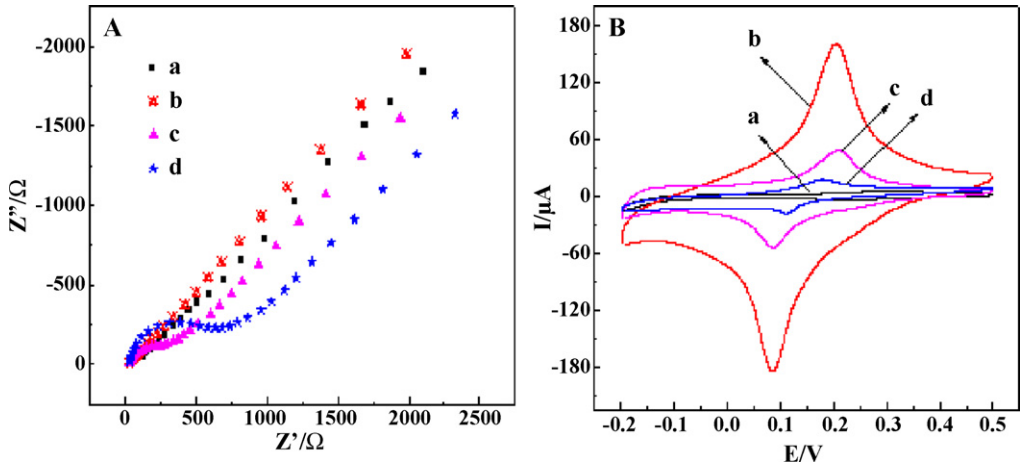

Fig. 3. (A) The electrochemical impedance spectroscopy (EIS) of different electrodes in 5.0 mM $[Fe(CN)_6]^{4-/3-}$ + 0.1 M KCl solution and (B) the cyclic voltammograms (CVs) of different electrodes in PBS (pH 6.0): (a) bare Au electrode; (b) CS–PB–MWNTs–H-PtCo/Au; (c) GOD/CS–PB–MWNTs–H-PtCo/Au and (d) Nafion/GOD/CS–PB–MWNTs–H-PtCo/Au. Scan rate: 100 mV s^{-1}.

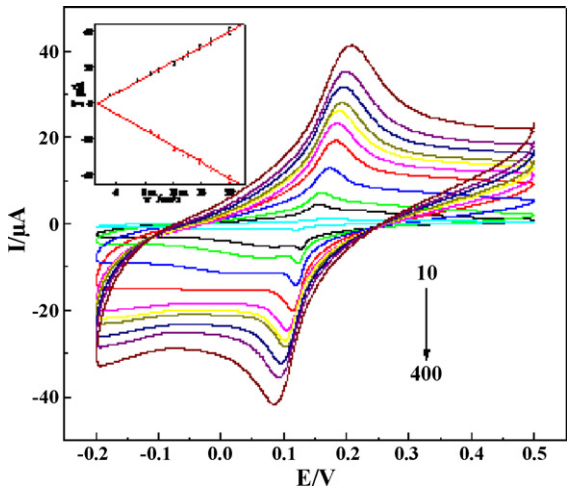

Fig. 4. The cyclic voltammograms (CVs) of Nafion/GOD/CS–PB–MWNTs–H-PtCo modified electrode at different scan rates: 10, 20, 50, 100, 150, 200, 300 and 400 mV s^{-1} in 0.025 M PBS (pH 6.0). The inset shows the dependence of redox peak currents on the square root of scan rates.

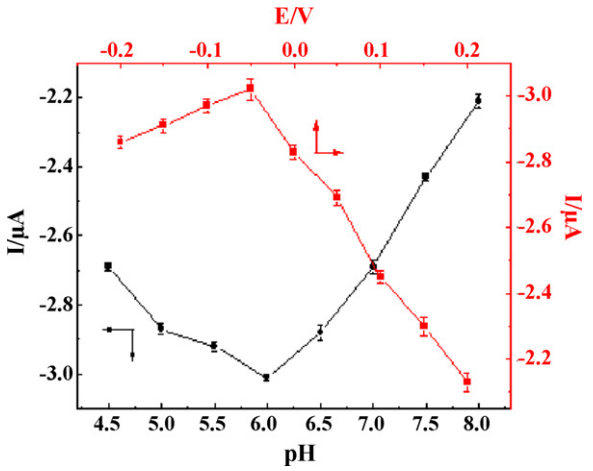

Fig. 6. Dependence of the current change of biosensor to 0.3 mM glucose on the pH of buffer solutions at an applied potential of −0.1 V and the applied potential in 0.025 M phosphate buffer solution (pH 6.0).

ite film was very satisfactory. Therefore, pH 6.0 phosphate buffer solutions were selected for the determination of glucose.

The dependence of chronoamperometric current response of the biosensor to constant concentration (0.3 mM) glucose on the applied potential from 0.2 to −0.2 V was investigated in pH 6.0 PBS (Fig. 6). The maximum response was reached at −0.1 V and it was selected as the working potential for further experiments. The effect of deposition time on electrocatalytic property of glucose biosensor was shown in Fig. 2S.

3.5. Amperometric response of the glucose biosensor

The amperometric response of the Nafion/GOD/CS–PB–MWNTs–H-PtCo/Au electrode was investigated by successively adding glucose to 5 mL stirred PBS solution under the optimized conditions. As controlled experiment, the amperometric responses were also measured at the Nafion/GOD/CS–PB/Au, Nafion/GOD/CS–PB–MWNTs/Au and Nafion/GOD/CS–PB–H-PtCo/Au electrodes with injecting the same concentration of glucose, respectively (Fig. 7A).

As can be seen, the Nafion/GOD/CS–PB/Au electrode showed a very small current response to glucose (curve a). Such response was mainly attributed to the synergic catalysis effects of PB and GOD molecule [31]. At the same time, both Nafion/GOD/CS–PB–MWNTs/Au (curve b) and Nafion/GOD/CS–PB–H-PtCo/Au (curve c) exhibited a relatively small response current to glucose. Whereas, drastic increase of the response current was observed at the Nafion/GOD/CS–PB–MWNTs–H-PtCo/Au electrode (curve d). This result demonstrated that the biosensor based on PB, MWNTs and hollow PtCo nanochains exhibited a better electrocatalytic activity to glucose ascribed to their synergistic action, since they had high surface area to entrap enzyme and excellent conductivity to promote the electron transfer.

In addition, to evaluate the electrocatalytic activity of the hollow and solid PtCo nanoparticles, the chronoamperometric response of the Nafion/GOD/CS–PB–MWNT–S-PtCo/Au electrode toward glucose was tested and the result was compared with those obtained on Nafion/GOD/CS–PB–MWNT–H-PtCo/Au electrode (Fig. 7B). The result revealed that the biosensor applied hollow PtCo had a better chronoamperometric response for glucose oxidation than using solid PtCo nanoparticles. The better catalyst was directly related to the high surface area of hollow nanoparticles.

The amperometric response of the target biosensor to successive addition of glucose was evaluated at −0.1 V under optimized conditions. The results were displayed in Fig. 8.

It was observed that the response time was very fast and the current value reached 95% steady-state response less than 5 s. The reason maybe that three-dimensional rough CS–PB–MWNT–H-

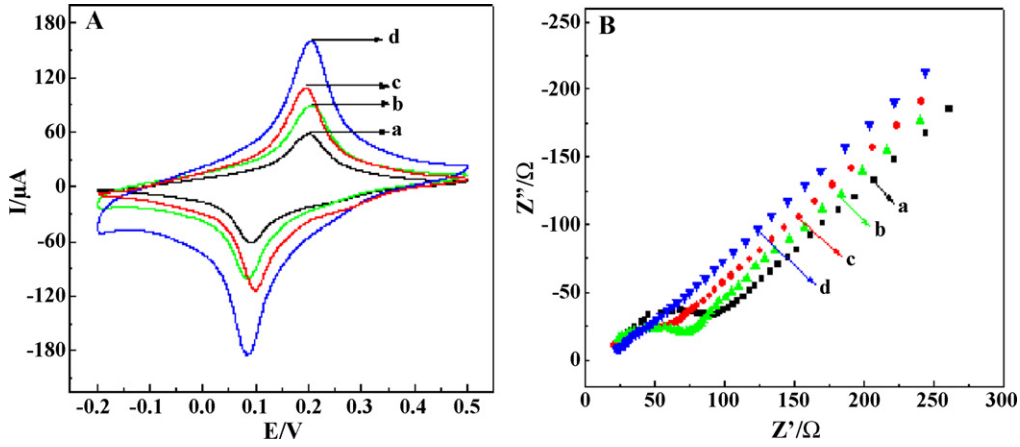

Fig. 5. The CV (A) and EIS (B) contrast test of the electrical conductivity (a) CS–PB/Au; (b) CS–PB–MWNTs/Au; (c) CS–PB–H-PtCo/Au and (d) CS–PB–MWNTs–H-PtCo/Au electrode.

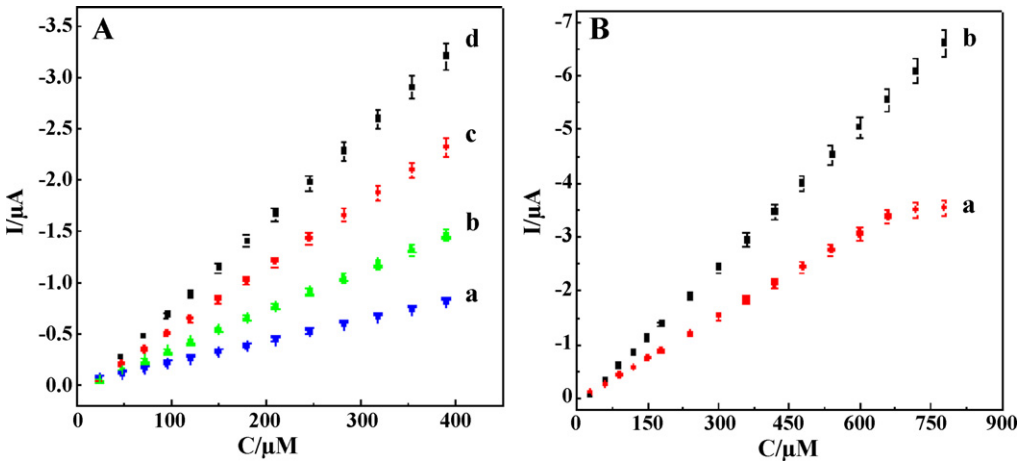

Fig. 7. (A) Amperometric response of (a) Nafion/GOD/CS–PB/Au; (b) Nafion/GOD/CS–PB–MWNTs/Au; (c) Nafion/GOD/CS–PB–H-PtCo/Au and (d) Nafion/GOD/CS–PB–MWNTs–H-PtCo/Au electrode in a stirred phosphate buffer solution (pH 6.0) after successive glucose additions at applied potential −0.1 V. (B) Amperometric response of (a) Nafion/GOD/CS–PB–MWNT–S-PtCo/Au and (b) Nafion/GOD/CS–PB–MWNT–H-PtCo/Au electrode in a stirred phosphate buffer solution (pH 6.0) after successive glucose additions at applied potential −0.1 V.

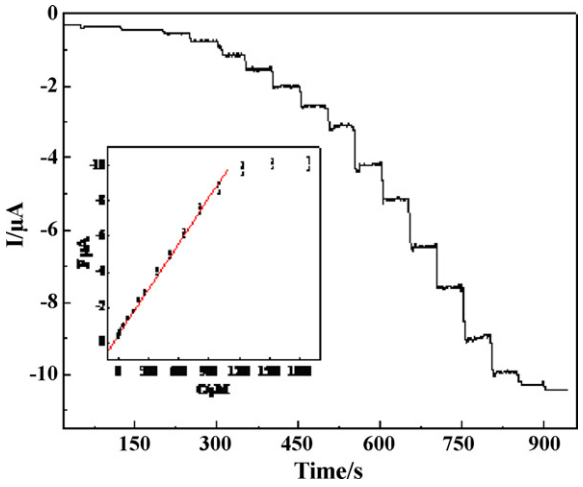

Fig. 8. Typical current–time response of the Nafion/GOD/CS–PB–MWNT–H-PtCo modified electrode on successive injection glucose into a stirred solution of 0.025 M phosphate buffer solution (pH 6.0) at applied potential −0.1 V. Inset: calibration curve of the biosensor.

PtCo film improved the conductivity and efficiently accelerated the electron transfer.

The corresponding calibration curve was shown in the inset of Fig. 8. The linear response range of the biosensor to glucose concentration was from 1.5 μM to 1.12 mM with a correlation coefficient of 0.9989, a detection limit of 0.47 μM (S/N = 3) and a sensitivity of 23.4 μA mM^{-1} cm^{-2}. The sensitivity was higher than that of 1.89 μA mM^{-1} cm^{-2} reported in Nafion/PBNPs film [8], 8.017 μA mM^{-1} cm^{-2} in the PB{Chi/MWNTs/GOD}$_6$ film [32], and 18 μA mM^{-1} cm^{-2} in PtPbNP/MWNT modified electrode [6]. When glucose concentration was higher than 1.6 mM, a response plateau was observed, showing the characteristics of the Michaelis–Menten kinetic mechanism. The apparent Michaelis–Menten constant (K_M^{app}), which gave an indication of the enzyme–substrate kinetics, can be obtained from the electrochemical version of the Lineweaver–Burk equation [33]:

$$\frac{1}{I_{ss}} = \frac{1}{I_{max}} + \frac{K_M^{app}}{I_{max}C}$$

where I_{ss} is the steady-state current after addition of substrate, I_{max} is the maximum current under saturated substrate condition and C is the bulk concentrate of the substrate. The K_M^{app} value for the Nafion/GOD/CS–PB–MWNT–H-PtCo modified electrode was determined to be 1.89 mM. The small value of K_M^{app} indicated that diffusion of substrate and product through the membrane was much easier in the Nafion/GOD/CS–PB–MWNT–H-PtCo film, and the proposed enzyme biosensor had a high biological affinity toward glucose [34].

In order to assess the analytical performance level of the proposed biosensor, the characteristics of the proposed biosensor were compared with other glucose biosensors, as shown in Table 1.

Results showed that the linearity range, detection limit and response time of the proposed biosensor were better than previously reported models. The favorable performances of the biosensor were attributed to the excellent conductivity and biocompatibility of CS–PB–MWNT–S-PtCo composite film. Meanwhile, there is a synergistic activity among PB, MWNTs and H-PtCo nanochains.

3.6. The mechanism of the electron-transfer behavior of the biosensor

The detailed catalytic process for the detection of glucose can be expressed in the following [35]. At first, glucose diffused from

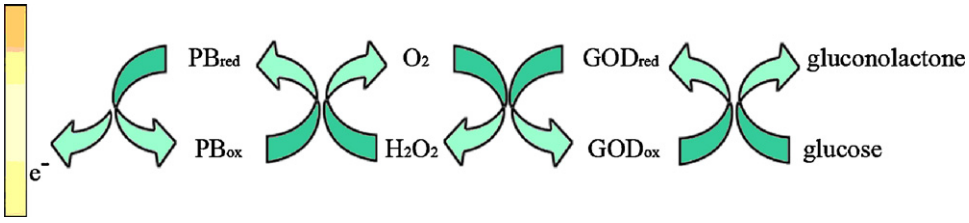

Fig. 9. Electrochemical response mechanism of the glucose biosensor.

Table 1
Electroanalytical characteristics of various modified electrodes toward glucose detection.

Electrode fabrication	Linearity range (mM)	Detection limit (μM)	K_M^{app} (mM)	Response time	Refs.
CS–Fc/MWNTs/GOD/GCE	0.02–5.36	6.5	6.87	10 s	[36]
CS–GOD/CS–PB/Au	0.002–0.4	0.397	3.37	10 s	[17]
CS–nano-Au–GOD/Nafion/Au	0.05–2.4	2.7	N/A	7 s	[37]
Nafion/GOD/Au_{nano}/Pt_{nano}/CNT/Au	0.5–16.5	400	10.73	7 s	[38]
Nafion/GOD/MWNTs/GCE	0.025–2.0	4.0	N/A	3 s	[39]
Nafion/GOD/MWNTs/GCE	0.001–0.5	1.3	9.8	N/A	[35]
Nafion/GOD/CS–PB–MWNTs–H-PtCo/Au	0.0015–1.12	0.47	1.89	4 s	This work

CS, chitosan; Fc, ferrocene; GOD, glucose oxidase; GCE, glass carbon electrode; Au, gold electrode; CNT, carbon nanotube; N/A, not available.

Table 2
Application of the biosensor for determination the recovery of glucose.

Sample	$C_{Original}$ (μmol L^{-1})	C_{Added} (μmol L^{-1})	C_{Found}[a] ± S.D. (μmol L^{-1})	R.S.D.%	Recovery (%)
1	5	1	6.1 ± 0.13	2.1	101.7
2	50	5	53.1 ± 0.96	1.8	96.5
3	100	10	107.4 ± 1.29	1.2	97.6
4	300	50	364.5 ± 6.12	1.7	104.1

[a] Mean value of five measurements.

the solution to the surface of the electrode, where it was enzymatically oxidized to give gluconolactone and H_2O_2 in the presence of oxygen.

$$\text{Glucose} + O_2 \rightarrow \text{Gluconolactone} + H_2O_2 \quad (1)$$

Second, Prussian white was then oxidized by the produced hydrogen peroxide to PB.

$$K_4Fe_4(II)[Fe(II)(CN)_6]_3 + 2H_2O_2 \rightarrow Fe_4(III)[Fe(II)CN_6]_3 + 4OH^- + 4K^+ \quad (2)$$

Third, the PB was subsequently reduced to Prussian white via electron exchange on the electrode surface.

$$Fe_4(III)[Fe(II)CN_6]_3 + 4e^- + 4K^+ \rightarrow K_4Fe_4(II)[Fe(II)(CN)_6]_3 \quad (3)$$

The whole process was very rapid. With the series of reactions circulated continuously, an electric current response was induced and quantitatively detected on the modified electrode. The mechanism of the process is schematically illustrated in Fig. 9.

3.7. Selectivity of the biosensor

The coelectrooxidation of potential interferences such as ascorbic acid and uric acid was one of the problems in the amperometric detection of analyte. The amperometric responses at the Nafion/GOD/CS–PB–MWNT–H-PtCo/Au electrode to the addition of five interfering substances (dopamine, glycine, L-cysteine, ascorbic acid and ethanol) in 0.025 M phosphate buffer solution (pH 6.0) at −0.1 V were shown in Fig. 10.

There was no significant change of the response current to be observed after the additions of interfering substances. The result demonstrated that the obtained biosensor had high selectivity for glucose determination, which was largely attributed to the low working potential and the additional Nafion layer coated on the biosensor.

3.8. Reproducibility and stability of the biosensor

The reproducibility of the proposed biosensor was also studied. The relative standard deviation (RSD) of the biosensor responsed to 0.3 mM glucose was 3.3% for five successive measurements. And the RSD for electrode-to-electrode reproducibility of five electrodes measured under the same conditions was 4.8%. The biosensors were stored at 4 °C when not in use and measured at intervals. There were not obvious changes of amperometric response during the first 3 days. After storage of two weeks and a month, the biosensors retained 92.1% and 85.3% of its original sensitivity. There are three reasons for this good stability and reproducibility. Firstly, CS had excellent film-forming ability. Thus, the PB coexisted with CS, MWNTs and hollow PtCo can effectively prevent PB leakage from the electrode. Secondly, the presence of MWNTs and hollow PtCo nanoparticles improved the electron-transfer and enhanced the enzyme loading owning to the formed three dimensional rough composite film. Thirdly, Nafion layer provided a very suitable microenvironment for enzyme entrapment and retained its activity.

3.9. Recovery experiment

The applicability of the proposed biosensor was valuated for detecting glucose concentration by standard addition method (Table 2).

The biosensor showed satisfactory results, with the recovery rate in the range 93.8–103%. The satisfying results demonstrated that the biosensor had a great potential for practical application.

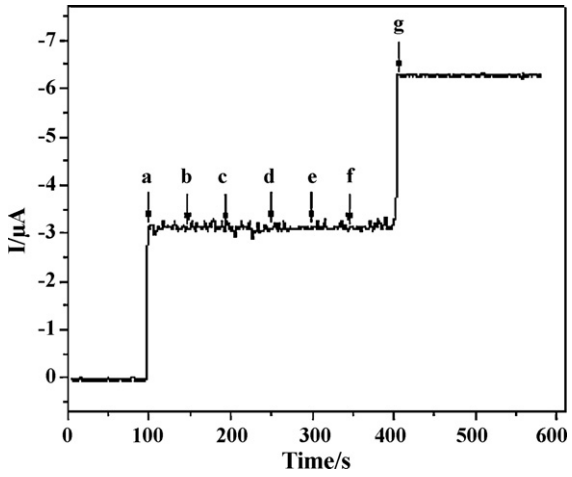

Fig. 10. Interference study by successive additions of (a) 0.3 mM glucose, (b) 0.6 mM ascorbic acid, (c) 0.6 mM L-cysteine, (d) 0.6 mM dopamine (e) 0.6 mM uric acid, (f) 0.6 mM glycine (g) 0.3 mM glucose in 0.1 M phosphate buffer solution (pH 6.0) at Nafion/GOD/CS–PB–MWNTs–H-PtCo modified electrode at an applied potential of – 0.1 V (vs. Ag/AgCl).

4. Conclusion

The CS–PB–MWNT–H-PtCo composite film had been successfully fabricated with the one-step electrochemical co-deposition method. Incorporating MWNTs and H-PtCo into CS–PB hybrid film constructed a three dimensional rough microstructure which increased the electron transfer relative to pure CS–PB films. Meanwhile, the composite exhibited a better amperometric response than using PB alone. Because of the synergistic effects between the MWNTs, H-PtCo nanochains and PB, the biosensor showed excellent performance in the merits of high sensitivity, good stability and reproducibility, wide linear response range, short response time and strong anti-interference ability. This method can be used in the preparation of other amperometric enzyme biosensors.

Acknowledgments

This work was supported by the National Natural Science Foundation of China (20675064), the Ministry of Education of China (project 708073), the Natural Science Foundation of Chongqing City (CSTC-2009BA1003), China and High Technology Project Foundation of Southwest University (XSGX 02), China.

Appendix A. Supplementary data

Supplementary data associated with this article can be found, in the online version, at doi:10.1016/j.colsurfb.2011.01.041.

References

[1] R.B. Rakhi, K. Sethupathi, S. Ramaprabhu, J. Phys. Chem. B 113 (2009) 3190.
[2] X.H. Kang, Z.B. Mai, X.Y. Zou, P.X. Cai, J.Y. Mo, Anal. Biochem. 369 (2007) 71.
[3] S.B. Bankar, M.V. Bule, R.S. Singhal, L. Ananthanarayan, Biotechnol. Adv. 27 (2009) 489.
[4] J.Y. Chiu, C.M. Yu, M.J. Yen, L.C. Chen, Biosens. Bioelectron. 24 (2009) 2015.
[5] S. Hrapovic, J.H.T. Luong, Anal. Chem. 75 (2003) 3308.
[6] H.F. Cui, J.S. Ye, W.D. Zhang, C.M. Li, J.H.T. Luong, F.-S. Sheu, Anal. Chim. Acta 594 (2007) 175.
[7] Y.Q. Lin, K. Liu, P. Yu, L. Xiang, X.C. Li, L.Q. Mao, Anal. Chem. 79 (2007) 9577.
[8] B. Haghighi, H. Hamidi, L. Gorton, Sens. Actuators B: Chem. 147 (2010) 270.
[9] S. Vaucher, M. Li, S. Mann, Angew. Chem. Int. Ed. 39 (2000) 1793.
[10] T. Uemura, S. Kitagawa, J. Am. Chem. Soc. 125 (2003) 7814.
[11] J.D. Qiu, R. Wang, R.P. Liang, X.H. Xia, Biosens. Bioelectron. 24 (2009) 2920.
[12] Y.M. Tan, W.F. Deng, C. Chen, Q.J. Xie, L.H. Lei, Y.Y. Li, Z.F. Fang, M. Ma, J.H. Chen, S.Z. Yao, Biosens. Bioelectron. 25 (2010) 2644.
[13] F. Ricci, G. Palleschi, Biosens. Bioelectron. 21 (2005) 389.
[14] H. Yi, L.Q. Wu, W.E. Bentley, R. Ghodssi, G.W. Rubloff, J.N. Culver, G.F. Payne, Biomacromolecules 6 (2005) 2881.
[15] R. Fernandes, L.Q. Wu, T.H. Chen, H. Yi, G.W. Rubloff, R. Ghodssi, W.E. Bentley, G.F. Payne, Langmuir 19 (2003) 4058.
[16] L.Q. Wu, H. Yi, S. Li, G.W. Rubloff, W.E. Bentley, R. Ghodssi, G.F. Payne, Langmuir 19 (2003) 519.
[17] X.Y. Wang, H.F. Gu, F. Yin, Y.F. Tu, Biosens. Bioelectron. 24 (2009) 1527.
[18] D.W. Wei, Y.Z. Ye, X.P. Jia, C. Yuan, W.P. Qian, Carbohydr. Res. 345 (2010) 74.
[19] M. Diaconu, S.C. Litescu, G.L. Radu, Sens. Actuators B: Chem. 145 (2010) 800.
[20] W. Zhao, H.C. Wang, X. Qin, X.S. Wang, Z.X. Zhao, Z.Y. Miao, L.L. Chen, M.M. Shan, Y.X. Fang, Q. Chen, Talanta 80 (2009) 1029.
[21] I. Baravik, R. Tel-Vered, O. Ovits, I. Willner, Langmuir 25 (2009) 13978.
[22] T.W. Tsai, G. Heckert, L.F. Neves, Y.Q. Tan, D.Y. Kao, R.G. Harrison, D.E. Resasco, D.W. Schmidtke, Anal. Chem. 81 (2009) 7917.
[23] J. Wang, Analyst 130 (2005) 421.
[24] S.F. Liu, J. Liu, X.P. Han, Y.N. Cui, W. Wang, Biosens. Bioelectron. 25 (2010) 1640.
[25] K. Kamata, Y. Lu, Y. Xia, J. Am. Chem. Soc. 125 (2003) 2384.
[26] C.E. Fowler, D. Khushalani, S. Mann, J. Mater. Chem. 11 (2001) 1968.
[27] M.M. Wu, G.G. Wang, H.F. Xu, J.B. Long, F.L.Y. Shek, S.M.F. Lo, I.D. Williams, S.H. Feng, R.R. Xu, Langmuir 19 (2003) 1362.
[28] Y. Vasquez, A.K. Sra, R.E. Schaak, J. Am. Chem. Soc. 127 (2005) 12504.
[29] Y.M. Zhai, J.F. Zhai, S.J. Dong, Chem. Commun. 7 (2010) 1500.
[30] X.Z. Cui, J.L. Shi, L.X. Zhang, M.L. Ruan, J.H. Gao, Carbon 47 (2009) 186.
[31] M.H. Xue, Q. Xu, M. Zhou, J.J. Zhu, Electrochem. Commun. 8 (2006) 1468.
[32] Y.J. Zou, C.L. Xiang, L.X. Sun, F. Xu, Electrochim. Acta 53 (2008) 4089.
[33] R.A. Kamin, G.S. Wilson, Anal. Chem. 52 (1980) 1198.
[34] M.M. Rahman, A. Umar, K. Sawada, Sens. Actuators B: Chem. 137 (2009) 327.
[35] H. Ohnuki, T. Saiki, A. Kusakari, H. Endo, M. Ichihara, M. Izum, Langmuir 23 (2007) 4675.
[36] R.P. Liang, L.X. Fan, R. Wang, J.D. Qiu, Electroanalysis 21 (2009) 1685.
[37] X.L. Luo, J.J. Xu, Y. Du, H.Y. Chen, Anal. Biochem. 334 (2004) 284.
[38] X. Chu, D.X. Duan, G.L. Shen, R.Q. Yu, Talanta 71 (2007) 2040.
[39] Y.C. Tsai, S.C. Li, J.M. Chen, Langmuir 21 (2005) 3653.